EXPERIMENTAL STUDIES OF ELECTRON MULTIPACTING IN CESR TYPE RECTANGULAR WAVEGUIDE COUPLERS*

R.L. Geng†, S. Belomestnykh, H. Padamsee, J. Reilly, LNS, Cornell Univ., Ithaca, NY14850, USA
P. Goudket‡, D.M. Dykes, ASTeC, CLRC DL, Warrington, UK
R.G. Carter, Lancaster University, Lancaster, UK

Abstract

We present experimental results obtained from stand-alone waveguide sections designed to test multipacting in CESR type rectangular waveguide couplers. We found that multipacting started at about 30 kW when the RF power was initially applied. Multipacting below 180 kW can be eliminated by RF processing. However, above 180 kW it persists even after an extended processing period. The effect of multipacting is found to be dependent on the RF pulse length. In short pulse (2 ms range) mode it is essentially harmless; but in longer pulse (20 ms range) or CW mode it induces gaseous discharge and hence trips power transmission. The concept of a slotted waveguide was tested and proven beneficial. The complete multipacting suppression is realized with the magnetic bias technique, for which a 10 Gauss bias field suffices.

1 INTRODUCTION

Rectangular waveguide couplers are widely used in superconducting, as well as normal conducting, RF systems for feeding power into RF resonators. Examples of such applications include colliders like CEBAF, CESR and PEP-II, as well as light sources such as SRRC, DIAMOND and CLS. With the increasing demands for beam power and system stability, the performance of RF couplers becomes critical to the smooth operation of these machines. Multipacting is an outstanding problem in RF couplers, that can cause failure if not properly addressed.

Presented in this paper is the study of multipacting in a waveguide section. This waveguide multipacting scenario was recently suspected to be responsible for the coupler related RF trips in CESR superconducting RF system [1]. Insight into the waveguide multipacting was gained through calculations with the computer code Xing [2]. It was shown that there exists higher order two-surface multipacting, the impact energy being in the range of 100 to 1000 eV. With the aid of the code, the DC magnetic bias technique and the slotted-waveguide concept were proposed to suppress multipacting in the waveguide coupler of SRF modules for CESR [3].

We have designed and built two waveguide sections of CESR type, one regular and one with a slot on a broad wall, to verify simulation predictions and further extend the understanding of waveguide multipacting.

* Work supported by the National Science Foundation.
† rg58@cornell.edu
‡ p.goudket@dl.ac.uk

2 EXPERIMENTAL APPARATUS

Fig. 1 illustrates the test waveguide along with the associated diagnostics. This 18" × 4" stainless steel test waveguide, is sandwiched between two taper waveguides, which in turn connect to standard WR1800 waveguides leading to the up-stream-end klystron and down-stream-end RF load. Two Mylar windows are inserted between the test waveguide and the tapers. A 50 L/s turbo pump attached to the narrow wall provides a baseline vacuum in the mid-10^{-6} Torr range. The RF power is provided by a 600 kW Philips YK1300 klystron. The diagnostics include four electron pick-up probes (P1 through P4), one photo-multiplier tube (PMT), one electron energy analyzer (EEA)[4], one cold cathode gauge, and several thermo-couples. The PMT signals (peak and average) and vacuum signals are also fed into an interlock system. Partial or full reflection is obtained by inserting an inductive iris or a shorting plate between the flanges of the down-stream-end taper and the adjacent WR1800 waveguide.

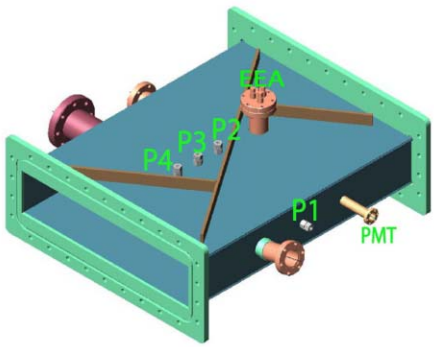

Figure 1: The multipacting test waveguide with associated diagnostics including electron probes P1 through P4, the electron energy analyzer EEA and the PMT.

3 RESULTS

3.1 Existence of Multipacting

The existence of multipacting is best demonstrated by the detection of a current by the three electron probes, P2, P3 and P4, placed along the center line of one of the two broad walls.

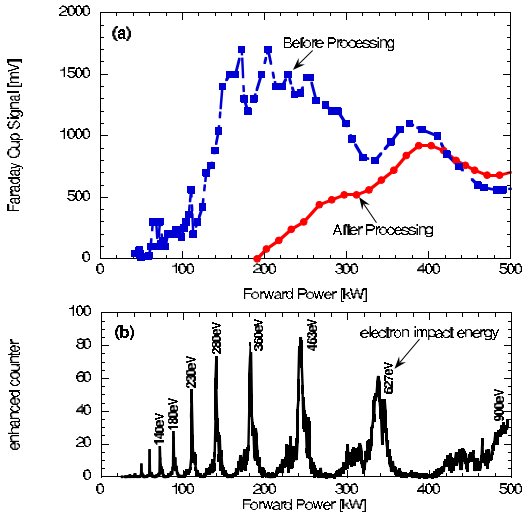

Figure 2: (a) Multipacting current before and after processing. (b) Calculated multipacting bands. The calculated electron impact energy is shown also.

3.2 *Processing*

For a reason that will become clear later, most studies were conducted in the pulsed mode (pulse length $\sim$ 2 ms). When the RF power was initially applied, strong electronic activities accompanied by strong vacuum and light activities were detected. Ramping the power has to be performed in a step by step manner because of many breakdown events that trip the system due to PMT light. This procedure is similar to RF processing. For an unbaked waveguide, multipacting starts at power levels as low as 30 kW; With the help of RF processing, power can be ramped up ultimately to the 600 kW range. Processing difficulty increases when a multipacting barrier is encountered.

After RF processing, multipacting below 180 kW is completely eliminated, as demonstrated in Fig. 2 (a). This processing effect is presumably a result of reduction for the secondary electron emission coefficient due to electron bombardment, which is most pronounced for lower impact energy. Calculations (Fig. 2(b)) show the corresponding impact energy is $<$ 360 eV for power levels below 180 kW. Multipacting currents for higher power levels change little even after further aggressive processing.

3.3 *Power Scanning and Multipacting Bands*

Systematic power scanning is performed after processing to map out the multipacting band structure. Fig. 3 depicts the multipacting bands for the traveling wave mode, as well as standing wave and mixed wave mode. As one can see, the multipacting current bears a non-zero value for all power levels above the onset threshold. Multipacting onset comes earlier at higher reflection ratios and the band structure is most evident for the traveling wave mode.

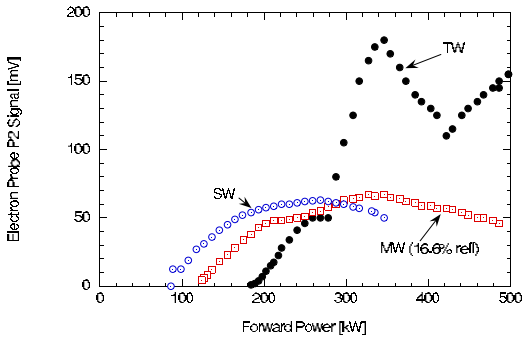

Figure 3: Multipacting bands for the traveling wave (TW) mode, standing wave (SW) mode, and mixed wave (MW) mode with a 16.6% reflection ratio.

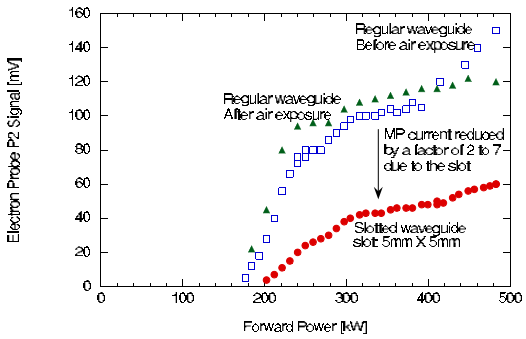

Figure 4: Suppression of multipacting by a 5mm wide slot opened along the high E field region of the broad wall.

3.4 *Suppressing Multipacting*

Fig. 4 illustrates the effect of a 5 mm wide slot opened along the center-line of the broad wall which lies opposite to the probes. A factor of 2 to 7 reduction in multipacting current is obtained. The beneficial effect of the slot is also evident during the processing period. Processing becomes much quicker above 180 kW; while for a regular waveguide, quick processing comes much later, at 270 kW.

Fig. 5 depicts the effect of a longitudinal DC magnetic field. Complete multipacting suppression is realized

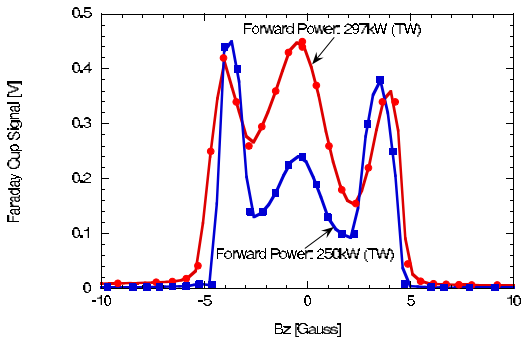

Figure 5: The effect of a magnetic bias field on multipacting current. Complete suppression is realized above a critical field value.

with both bias polarities. This technique is effective up to 550 kW, for which a 10 Gauss bias field suffices. Multipacting is enhanced at a bias field slightly smaller than the suppression field. This effect is attributable to the oblique incidence of impacting electrons, whose orbit is bent due to the bias magnetic field. By associating the cyclotron radius of multipacting electrons with the narrow dimension of the waveguide, we have derived an analytical formula for the suppression bias field Bz^*, which is given by $Bz^* = \sqrt{\frac{4\mu_0 P_f}{k\omega a b^3}}$, where P_f is the forward power, k the wave propagation constant, μ_0 the permeability of vacuum, ω the angular RF frequency, a and b the wide and narrow dimension of the waveguide respectively.

Multipacting suppression coils have been in operation in the CESR cryomodule installed in the E1 position since July 2001. We use a bias coil on the waveguide portion that is outside magnetic shielding of the cryostat. The bias field is about 10 Gauss. The result is positive and in the long term we did not see any adverse effects on the performance of the superconducting RF cavity due to the bias magnetic field.

4 DISCUSSION

A comparison between the experimental results and the previous simulation results has been made. Reasonably good agreement exists for the band positions, as well as for the impact energies. The code's results were however much more clear-cut than what was observed, probably due to the simplified mechanisms that the code uses. The experiment revealed valuable information about the effect of processing and of pulse length, for which models need to be developed.

4.1 Processing Effect

During the initial processing period, the waveguide pressure increase closely follows the electron current, typically reaching the high-10^{-5} Torr range. Light activity may be detected on the PMT and is a precursor to vacuum breakdown. After sitting at the power level for a variable time (dependent on the hardness of the multipacting band), the electron current becomes essentially stable (but not nil) and waveguide pressure begins to recover. No light is visible on the PMT at this stage. These observations can be explained by gas desorption stimulated by the multipacting electrons, which can then lead to a gas discharge breakdown.

Gas exposure tests have been done to check if the processing effect is preserved. The multipacting current was slightly enhanced after a 5-minute exposure to filtered N2 gas. In contrast, the processing effect was completely lost after an air exposure.

4.2 Pulse Length Effect

The RF pulse length has a large effect. In the short pulse (2 ms range) mode, the multipacting current is self-sustained for reasons that are not yet understood. No change in reflected power can be measured. Multipacting in these conditions is essentially harmless.

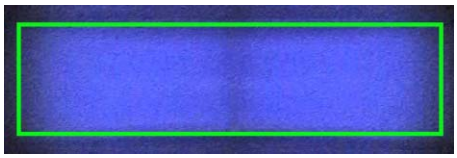

Figure 6: Multipacting induced discharge. The rectangular box outlines the waveguide boundary. The central dark zone is observed for a slotted-waveguide.

However, with a longer pulse (20 ms range) or in CW mode, the initial self-sustained multipacting finally develops into an exponential increase of the electronic current accompanied by an increase of waveguide pressure to the mid-10^{-4} Torr range. Some reflected power can be measured in this case. This electron avalanche is also accompanied by whitish-blue light, which is visible through the Mylar windows. Interestingly, a dark zone was observed for a slotted-waveguide (see Fig. 6), as opposed to a brighter zone for a regular waveguide. The electron energy analyzer reveals a large fraction of low energy electrons during such activities. By reversing the bias polarity of the electron probe, a current due to positively charged particles can be measured. These observations suggest that the direct cause of RF transmission breakdown is due to gaseous discharge, resulting from the impact ionization between multipacting electrons and the desorbed gas molecules. For this reason, gas desorption is as important as secondary electron emission when addressing multipacting in an RF power coupler. Ideal waveguide material or surface coatings should possess both a low secondary electron emission coefficient and a low electron-stimulated gas desorption yield. Pumping capacity should also be maximized in the coupler region to reduce gas density and hence to reduce the ionization rate.

5 CONCLUSION

Multipacting can be eliminated by RF processing only for lower power levels. At higher power levels, it persists even after an extended processing period. In short pulse (2 ms range) mode, multipacting is essentially harmless; but in longer pulsed operation ($>$ 20 ms range) or CW mode it induces gaseous discharge and hence inhibits the RF transmission. The slotted-waveguide concept has been shown to be beneficial. Complete multipacting suppression can be realized with a bias magnetic field of 10 Gauss, low enough to not adversely affect the performance of superconducting cavities.

6 REFERENCES

[1] S. Belomestnykh et. al., PAC 1999, P.980.

[2] R.L. Geng, H. Padamssee, PAC 1999, P.429.

[3] R.L. Geng, H. Padamsee, V. Shemelin, PAC 2001, P.1228.

[4] R.A. Rosenberg, K.C. Harkay, NIM A 453(2000)507-513.